

## Dynamical stability of the crack front line

Takayasu FUKUHARA\* and Hiizu NAKANISHI

*Department of Physics, Kyushu University 33, Fukuoka 812-8581*

(Received Jun. 1, 1998)

Dynamical stability of the crack front line that propagates between two plates is studied numerically using the simple two-dimensional mass-spring model. It is demonstrated that the straight front line is unstable for low speed while it becomes stable for high speed. For the uniform model, the roughness exponent in the slower speed region is fairly constant around 0.4 and there seems to be a rough-smooth transition at a certain speed. For the inhomogeneous case with quenched randomness, the transition is gradual.

KEYWORDS: crack propagation, dynamical instability, crack front roughening, rough-smooth transition

---

\* Present address: Mikuniya Corp. 1-1-20, Toranomon-Jitsugyokaikan Bld. Toranomon, Minato-ku, Tokyo 105, Japan,

## §1. Introduction

It has been known for a long time that the straight and smooth crack propagation becomes unstable under certain circumstances. The “mirror–mist–hackle” transition of the crack surface of glass rod<sup>1)</sup> is one of the manifestation of the instability that the crack surface becomes rougher as the crack speed increases. A much more controlled experiment that is related to the instability has been done on the fracture propagation in the PMMA glass plate,<sup>2)</sup> and the smooth crack propagation was found to become unstable beyond a certain crack speed around 60% of Rayleigh speed.

On the other hand, there could be another instability in other direction, namely, “in-plane” crack front instability. In the three dimensional crack propagation, the crack front line within the plane of crack surface could be rough under certain circumstances. The experiment to observe the crack front roughness was done first by Daguer *et al.*<sup>3)</sup> on very slow crack in metal alloys, and they found the in-plane crack front roughness exponent to be  $0.51 \sim 0.64$ .

Schmittbuhl and Måløy<sup>4)</sup> observed the time development of the in-plane crack front that propagates between the two Plexiglas plates annealed together. They found the crack front shows self-affine rough structure with the exponent  $0.55 \pm 0.05$  for the crack speed much slower than the sound speed;  $5 \times 10^{-5} m/s$ .

There are some theoretical approaches to the above instability: Schmittbuhl *et al.*<sup>5)</sup> studied the quasi-static dynamics driven by the stress intensity factor along the crack front under the existence of quenched randomness. They found from numerical simulations the roughness exponent  $\alpha = 0.35$  and the dynamic exponent  $z = 1.5$ ; these exponents are quite different from those for the local dynamics, and the difference was attributed to the long range interaction through stress field.

Ramanathan *et al.*<sup>6)</sup> studied the roughness exponents for the surface under the similar situations, and found the surface roughness exponent is  $1/2$  for mode III loading, but the surface is only logarithmically rough for mode I due to the long range interaction.

In the present paper, we study the in-plane crack front stability using the two dimensional mass-spring model when the crack speed is comparable with the sound speed; the situation is quite different from most of other experimental and theoretical works, where the quasi-static case was investigated.

Organization of the paper is as follows: The model is defined in §2, and the uniform propagating solution is described in §3. The method and results of the numerical simulations for the two version of the model are given in §4, and the summary and discussion in §5.

## §2. Model

The model we study is a 2-d version of the 1-d model studied by Marder and Gross,<sup>7)</sup> but it is extended in the different sense from the 2-d model by Marder and Liu,<sup>8)</sup> namely, the system

consists of the two layers of triangular lattices and the two plates are attached to the system from the top and the bottom (Fig.1). The external stress is imposed by the displacement  $2U_N$  between the two plates and the crack is assumed to propagate along the  $y$  axis by breaking the springs that connects the two layers.

We simplify the model by assuming that the masses move only along the  $z$ -axis, and the displacement of the  $i$ -th mass in the upper layer is denoted by  $U_i$ . Assuming the symmetric motion for the upper and lower layer, we simulate only the upper part of the system; the displacements of the lower masses are  $-U_i$ . Then, the equation of motion we study is given by

$$m\ddot{U}_i = k_1(U_n - U_i) + k_2U_i\theta(U_{fi} - U_i) + \sum_{j \in n.n.} k_3(U_j - U_i) - b\dot{U}_i \quad (1)$$

for the mass in the upper layer. Note the factor 2 difference in the definition of  $k_2$  from the one in ref 7).

In the equation,  $m$  is the mass, and  $k_1$ ,  $k_2$ , and  $k_3$  are the spring constants that connect the  $i$ -th mass to the external plate, to the mass in the other layer, and to the nearest neighbor mass in the same layer, respectively. (Note that we assumed the linear force with the displacement difference for the spring  $k_3$  in eq.(1) although Fig.1 may seem to imply the third order dependence.)  $U_N$  is the external displacement imposed by the plates.  $\theta(x)$  is the step function and  $U_{fi}$  is the threshold displacement for breaking the  $i$ -th springs connecting the two layers.  $b$  is the small parameter for dissipation, which is introduced to dump the unwanted persistent oscillatory motion.

Note that the model is uniform except for the threshold  $U_{fi}$  for the spring  $k_2$ .

### §3. Uniform propagation

The analytic solution for the steady propagation in the 1-d version of the model has been obtained by Marder and Gross.<sup>7)</sup> They calculated the crack speed  $v$  as a function of the external displacement and pointed out some of its interesting features: The crack is trapped by the lattice and does not move even when the external displacement  $U_n$  exceeds the threshold value  $U_n^c$  for which the elastic energy store in the springs equals the energy needed to break the springs, namely, Griffith threshold, until  $\Delta \equiv U_n/U_n^c$  reaches a certain value larger than 1; then the crack speed jumps around 0.4 time the sound speed, therefore, there is a forbidden band of crack speed. (Fig.5. of ref 7))

In the present version of the 2-d model with the uniform threshold, the steady crack propagation shows the similar behavior: a lattice trap and a forbidden band of crack speed. Note that the uniform solution in the 2-d model need not behave exactly in the same way with the 1-d model unless we consider the crack propagation along the axis in the square lattice, because there is a diagonal interaction between neighboring rows.

In principle, it should be possible to do the similar analysis for the 2-d uniform solution as that

of Marder and Gross<sup>7)</sup> by assuming a certain periodicity of the solution, but we examine the uniform solution numerically because our main object of the present work is studying inhomogeneous behavior of the crack propagation.

The numerically obtained crack speed  $v$  as a function of the normalized external displacement is shown in Fig.2. The major difference from the 1-d case is that there is a “mid-gap band” in the middle of forbidden band in the  $v - \Delta$  plot. This should come from the interaction between rows; a broken bond helps to break the bond at the crack front in a neighboring row in the parameter region where the 1-d model does not have a propagating solution.

#### §4. Simulations and Results

In order to examine the dynamical stability of the fracture front and effects of inhomogeneity on it, we study two versions of the models. The first one, which we call the model A, is the model with uniform threshold  $U_{fi} = U_f$  for all the site  $i$  except for a single row parallel to the crack front. The row with random threshold is introduced to apply perturbation on the steady solution, and we examine how the perturbation will develop as the crack front propagates in the uniform region. The second one, the model B, is the model with random distribution of the threshold over the whole system.

We simulate the system behavior by integrating eq.(1) numerically using the modified Euler’s method; note that the modified Euler’s method itself is the method with the second order accuracy in the time step, but the error in linear with the time step can be introduced by the singularity of the term that represents breaking bonds.

We employ the unit where  $m = k_2 = 1$ , and in all of the simulations we take  $k_3 = k_2$ ,  $k_1 = 0.1$ , and  $b = 0.01$ . It is convenient to measure the external displacement by the ratio  $\Delta$ ,

$$\Delta \equiv U_n/U_n^c; \quad (2)$$

with  $U_n^c$  being a critical displacement where the elastic energy equals to the bond breaking energy;

$$U_n^c \equiv \frac{U_n}{\sqrt{1 + k_2/k_1} U_f}. \quad (3)$$

The boundary conditions we employ along the  $x$ -axis are periodic for the model A and “reflecting” for the model B; in the reflecting boundary condition, outside the system we add a virtual column which behaves in the same way as the column next to the boundary does. Along the  $y$ -axis, only the part of the system around the crack line is simulated, and new rows in front are added and rows left behind are discarded as the crack advances in order that the crack front is kept around the center of the simulated part; the length of the simulated part is taken as about twice of the width.

#### 4.1 Model A

Fig.5 shows the time development of the crack front for the model with the uniform threshold  $U_{fi} = 0.7$  except for a single impurity with  $U_{fi} = 1.0$  located in the 70'th row from the left side of the system where the crack starts. The external driving is  $\Delta = 1.049$ . It can be seen that the impurity causes disturbance which eventually develops over the whole system and results in the rough crack front.

In order to avoid distortion of the crack front, next we consider the perturbation by the impurity sites distributed over the 70'th row randomly; along the 70'th row, the value of threshold takes  $U_{fi} = 0.8$  with the probability 0.15, and  $U_{fi} = 0.7$  for the rest of the site. The results are shown in Fig.4 for  $\Delta = 1.049, 1.052$ , and  $1.053$ .

As the crack speed increases, it looks the “roughness” of the crack front decreases. The roughness exponents  $\alpha$  of the crack front for various values of  $\Delta$  are plotted in Fig.5. We used the Max-Min method<sup>9)</sup> to determine the roughness exponents, but we have also checked for some points that the power spectrum method gave the similar values. The roughness exponent  $\alpha$  for the “slow” crack is fairly constant and about 0.4, but the crack front becomes smooth and  $\alpha \sim 0$  for  $\Delta > 1.052$ , which roughly coincides with the end of the mid-gap band in Fig.2.

#### 4.2 Model B

In the model B, the impurity site with  $U_{fi} = 1.0$  is distributed over the whole system with the probability 0.09 and the rest of the sites has  $U_{fi} = 0.7$ . The time developments of the crack fronts are shown in Fig.6 for  $\Delta = 1.120, 1.129$ , and  $1.141$ . The roughness exponents  $\alpha$  of the front are  $\alpha = 0.67, 0.50$ , and  $0.35$ , respectively. The general trend that the front line is smoother for larger  $\Delta$  is the same with the case of model A, but the front line are substantially rougher for the model B and there is no clear transition to the smooth front as the model A.

As for the case of  $\Delta = 1.120$ , we also analyzed the time development of the crack front roughening using the finite size scaling. We measured the width of the front line  $W$  as a function of the system width  $L$  and the distance that the crack front travels  $X$ , and fit the data in the form,

$$W(L, X) \sim L^\alpha f\left(\frac{X}{L^z}\right), \quad (4)$$

where  $z$  is the dynamical exponent and  $f(x)$  is a scaling function,

$$f(x) \sim \begin{cases} x^\beta & (x \ll 1) \\ \text{const.} & (x \gg 1) \end{cases} \quad (5)$$

with  $\beta$  being the growth exponent and the scaling relation  $z = \alpha/\beta$  holds. The scaling plot is shown in Fig.7 with  $\alpha = 0.70$  and  $\beta = 1.4$  for  $L = 512, 256, 128$ , and  $64$ .

## §5. Discussion

We have studied the stability of crack front numerically using a simple 1-d mass-spring system, and found the straight crack front propagation is not stable especially for slower crack speed. This contrasts with the dynamical instability of the crack surface, where the instability takes place for higher speed.<sup>2,8)</sup>

For the uniform model perturbed by the localized impurities, there seems to be a rough-smooth transition at the certain speed beyond which the crack front becomes smooth. In the rough region at slower crack speed, the roughness exponent is fairly constant around 0.4.

For the inhomogeneous model where the bond breaking threshold is random, the front line also becomes smoother for the higher speed, but the transition from rough to smooth front is gradual. For the slowest case we simulated, the obtained exponent  $\alpha = 0.70$  is to be compared with 0.75 of the roughness exponent for the KPZ system with the quenched noise, or with 0.633 of the directed percolation.

On the other hand, however, the growth exponent  $\beta = 1.4$  and the dynamical exponent  $z = 0.5$ , which are related to the dynamical process, are quite different from those systems, where  $\beta = 0.61$  and  $z = 1.16$  for KPZ with the quenched randomness,<sup>10)</sup> and  $\beta = 0.633$  and  $z = 1$  for the directed percolation.<sup>11,12)</sup>

The experiment which is closely related to the present work has been done on the Plexiglas,<sup>4)</sup> and the exponent was found to be around  $0.55 \pm 0.05$ . This is not very different from the one we obtained for the uniform model, 0.4, but it should be noted that there are major differences in the experimental situations from the present calculation; 1) the crack speed in the experiment is  $10^{-7} \sim 10^{-5} m/s$  and much slower than the sound speed, 2) there should be some long range interaction due to the three dimensionality even though the experiment was done on the plate whose thickness is much smaller than the width.

## Acknowledgement

The work is partially supported by Grant-in-Aid for Scientific Research (c), the Ministry of Education, Science, Sports, and Culture (grant # 09640468), and the Hong Kong Research Grants Council Grant No. 315/96P.

- 
- [1] B.R. Lawn: *Fracture of brittle solid, 2nd edition*, Cambridge University Press, 1993.
  - [2] J. Fineberg, S. Gross, M. Marder, and H. Swinney: Phys. Rev. Lett. **67** (1991) 141; Phys. Rev. B **45** (1992) 5146.
  - [3] P. Daguerre, E. Bouchaud, and G. Lapasset: Europhys. Lett. **31** (1995) 367.
  - [4] J. Schmittbuhl and K.J. Måløy: Phys. Rev. Lett. **78** (1997) 3888.
  - [5] J. Schmittbuhl, S. Roux, J-P. Vilotte, and K.J. Måløy: Phys. Rev. Lett. **74** (1995) 1787.
  - [6] S. Ramanathan, D. Ertas, and D.S. Fisher: Phys. Rev. Lett. **79** (1997) 873.
  - [7] M. Marder and S. Gross: J. Mech. Phys. Solids, **43** (1995) 1.

- [8] M. Marder and X. Liu: Phys. Rev. Lett. **66** (1993) 2417.
- [9] J. Schmittbuhl, J-P. Vilotte, and S. Roux: Phys. Rev. E **51** (1995) 131.
- [10] D.A. Kessler, H. Levine, and Y. Tu: Phys. Rev. A **43** (1991) 4551.
- [11] L.-H. Tang and H. Leschhorn: Phys. Rev. A **45** (1992) R8309.
- [12] S.V. Buldyrev, A.-L. Barabási, F. Caserta, S. Havlin, H.E. Stanley, and T. Vicsek: Phys. Rev. A **45** (1992) R8313.

figure 1

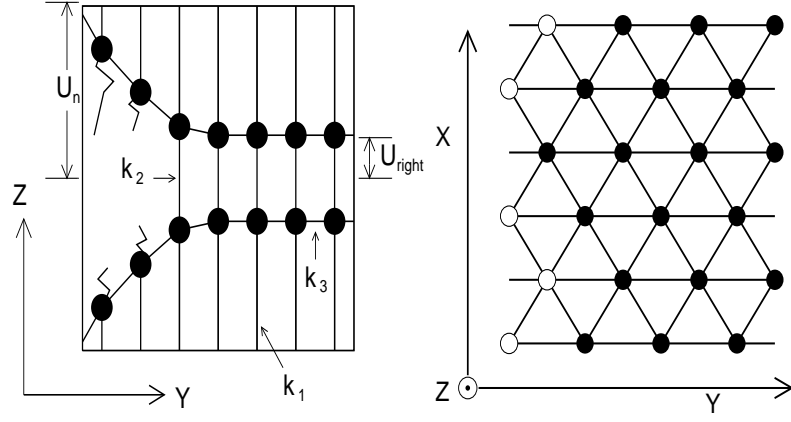


Fig. 1. Side(left) and top(right) view of the mass-spring system. In the top view, the open circles denote the broken bonds. Note that we assumed the linear force with the displacement difference for the spring  $k_3$  also in eq.(1).



figure 2

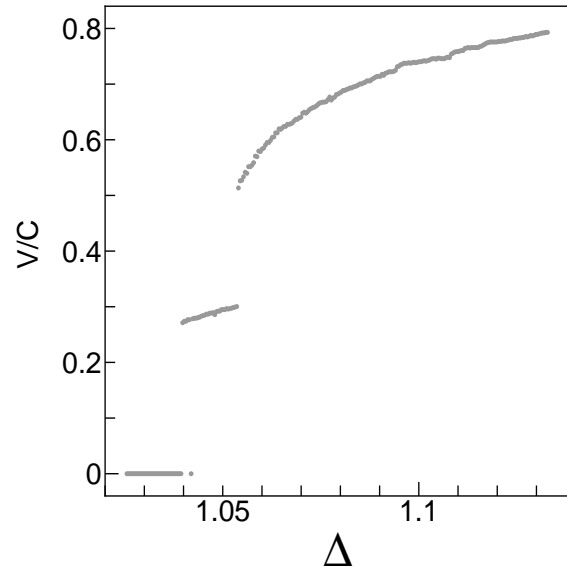


Fig. 2. Crack speed  $v$  *v.s.* external displacement  $\Delta$  for the uniform propagation.  $c$  denotes the sound speed.

figure 3

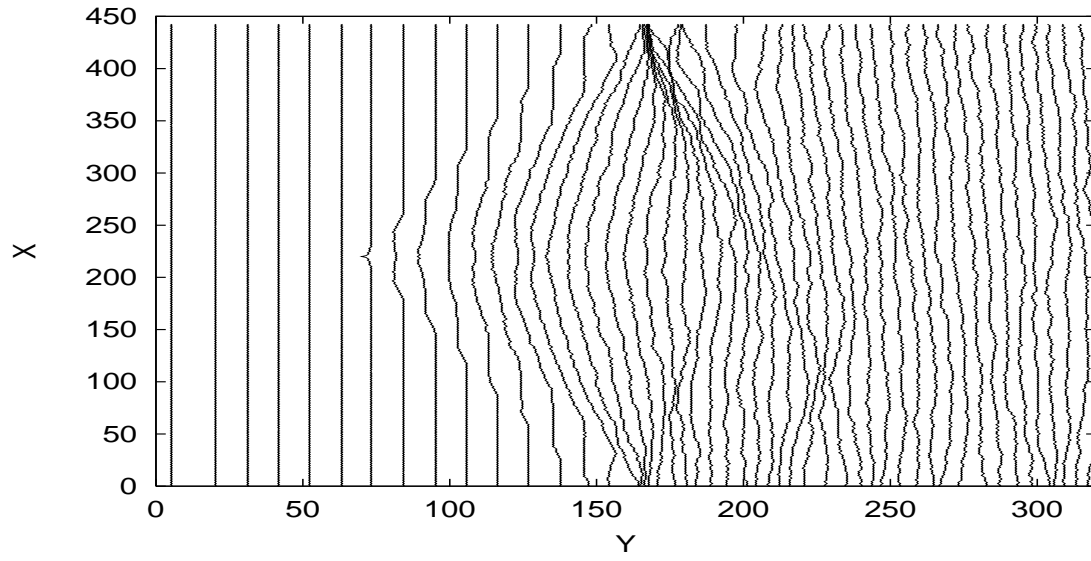


Fig. 3. Time development of the crack front. The steady solution is disturbed by a single impurity.

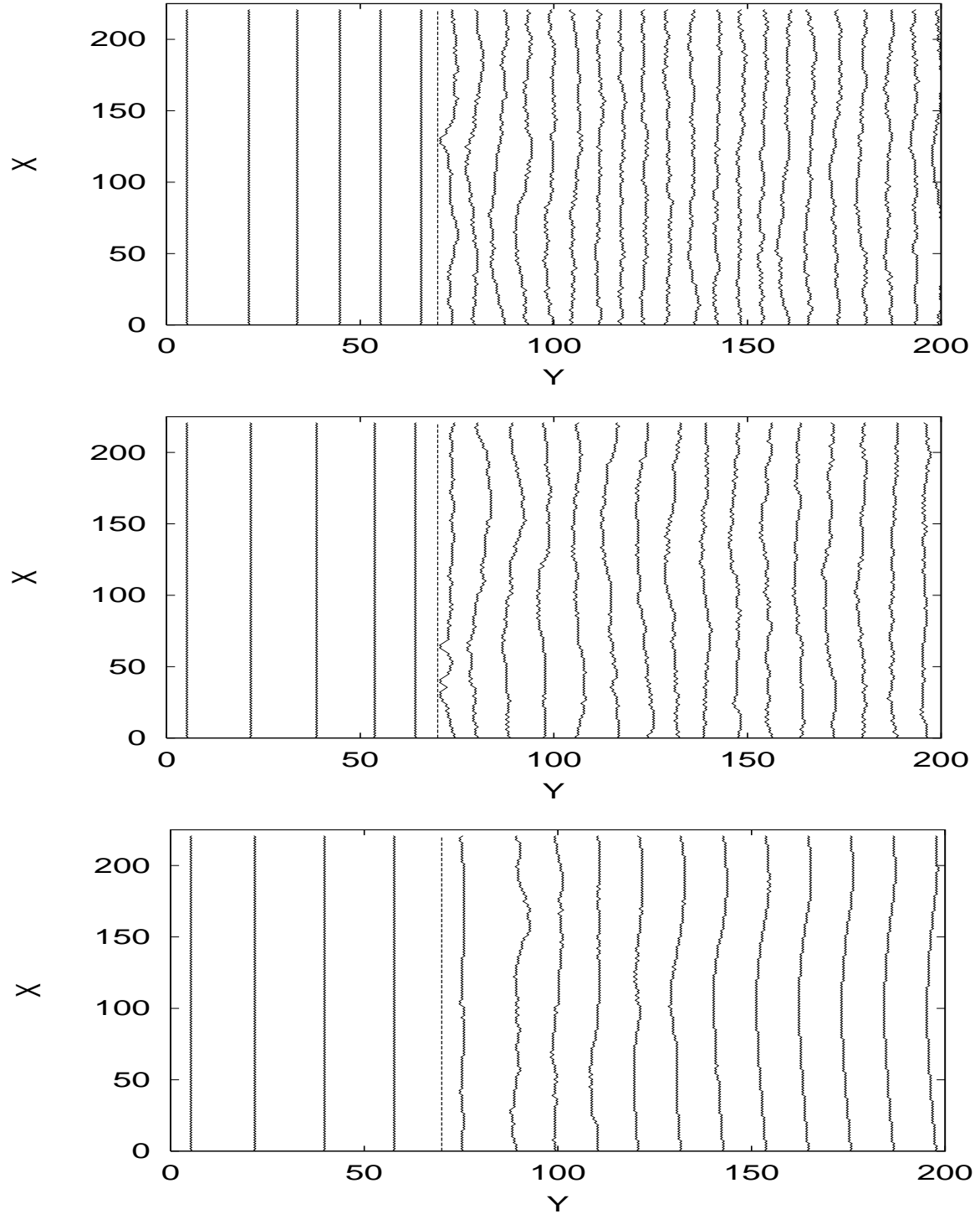


Fig. 4. Time developments of the crack front. The external displacements are  $\Delta = 1.049$  (top), 1.052 (middle), and 1.053 (bottom).

figure 5

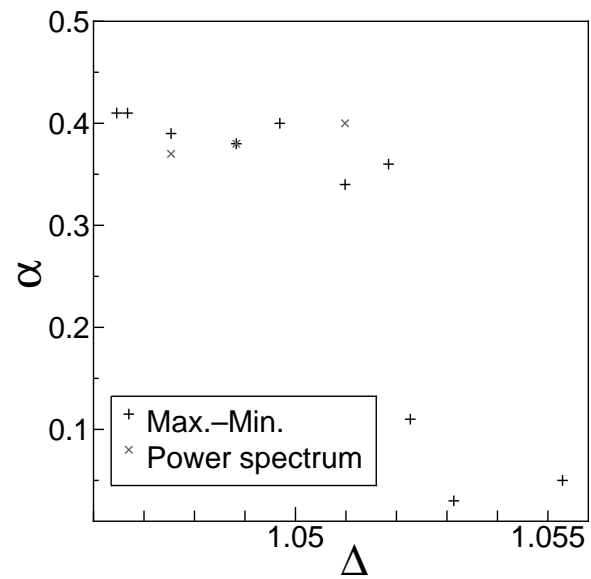


Fig. 5. Roughness exponents  $\alpha$  *v.s.* the external displacement  $\Delta$  for the model A.

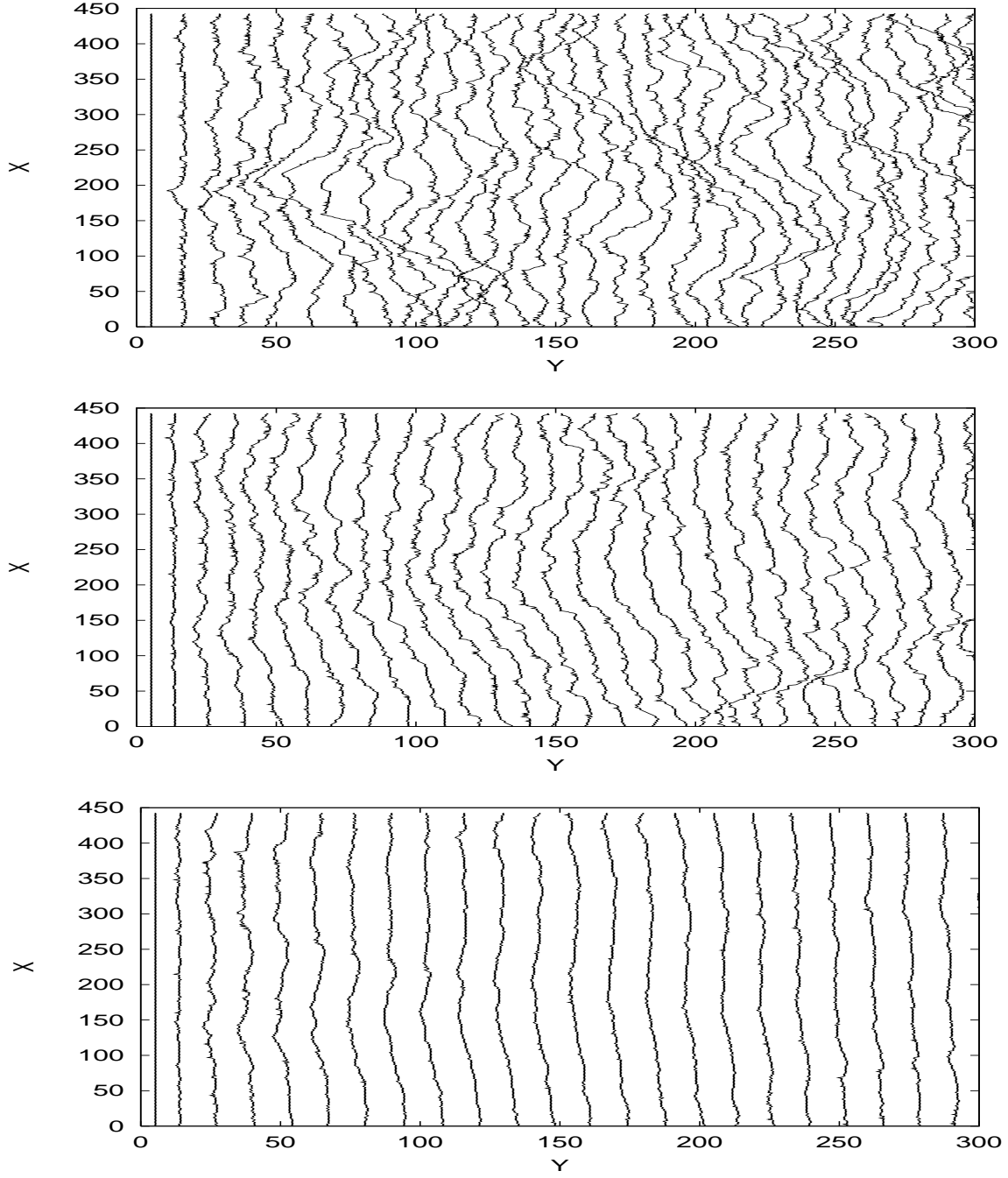


Fig. 6. Time development of the crack front for the model B. The external displacements are  $\Delta = 1.120$  (top), 1.129 (middle), and 1.141 (bottom).

figure 7

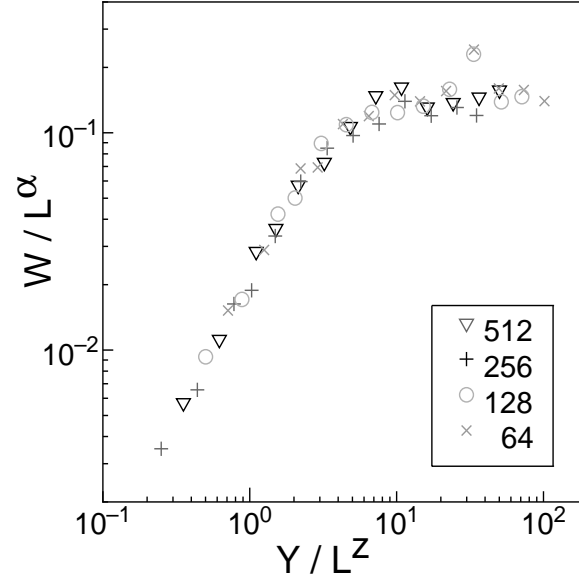


Fig. 7. Scaling plot for the time development of the crack front in the model B with  $\Delta = 1.120$ . The fitting parameters are  $\alpha = 0.70$  and  $\beta = 1.4$ .